MIRI Cooler System Design Update

M. Petach, D. Durand, M. Michaelian, J. Raab, and E. Tward

Northrop Grumman Aerospace Systems
Redondo Beach, CA 90278 USA

ABSTRACT

The Mid Infrared Instrument (MIRI) for the James Webb Space Telescope (JWST) requires cooling at 6 K for the SiAs focal planes, provided by an active cooler. The four stage cooler consists of: a three-stage pulse tube precooler, Joule Thompson (J-T) circulator and upper stage recuperators, located on the JWST spacecraft bus, and the final stage recuperator and 6 K J-T expander, located at the remote instrument module with a 12 meter round trip line at 18-22 K between the spacecraft and instrument. Since our last report on the cooler design, the JWST program has made design changes to the overall thermal design, including the addition by Goddard Space Flight Center (GSFC) of an actively cooled thermal shield surrounding the MIRI Optical Module to increase the overall thermal efficiency and thereby increase the margin between the cooler lift capability and the expected heat loads. This change shifts a portion of the thermal load from the 6 K cooler stage to the 18-22 K stage. Meeting the increased thermal load at 18-22 K and realizing the benefit from the decreased load at 6 K requires operating the cooler at a different set of operating points. In this paper, we report on the required changes to the cooler's operation and design, and demonstrate that the basic design has the capacity to meet the new requirements.

INTRODUCTION

The Mid Infrared Instrument (MIRI) Cooler Subsystem cools the MIRI focal plane arrays to their operating temperature of 6.7 K using a closed cycle helium Joule-Thomson cooler precooled by a three-stage pulse tube cryocooler. As described previously, [1-4] the MIRI Cooler design provides a 6.2 K remote cold head interface on the optical bench, near the focal plane modules. Much of the cooler hardware, including the Joule-Thomson compressor, the pulse tube precooler, and cooler drive/control electronics is located in the spacecraft bus, several meters from the instrument's Optical Module (OM). Figure 1 shows an updated functional block diagram of the MIRI Cooler. A heat exchanger has been added to the return path of the Joule-Thomson helium gas on the "18 K" side of the coldest recuperator to provide a thermal interface for the heat load from the actively cooled thermal shield surrounding the OM (see the dashed oval in Figure 1).

In terms of thermodynamic performance, the thermal load applied to the shield heat exchanger (SH HX) and parasitic load on the refrigerant return line, including the Refrigerant Line Deployment Assembly (RLDA), are essentially equivalent and the driving requirement is the total heat load on the nominally 18 K stage of the cooler. The cooler had been designed and tested to heat loads in the steady state of 68 mW at 6.2 K with a simultaneous load of 79 mW divided equally between the refrigerant supply and return lines. Changes in the MIRI/JWST cryogenic system design led to the current cooler requirements of 55 mW at 6.2 K and 232 mW total load on the

Cryocoolers 16, edited by S.D. Miller and R.G. Ross, Jr.

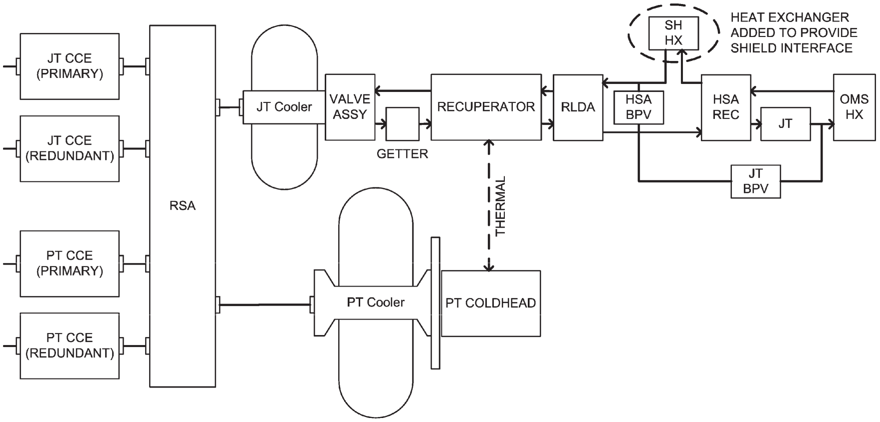

Figure 1. MIRI Cooler Subsystem Block Diagram as shown in Durand, et. al.,[4] except for the addition of the actively cooled shield heat exchanger "SH HX" shown in the dashed oval. "J-T" stands for Joule-Thomson, "CCE" stands for Cryocooler Control Electronics, "RSA" stands for Relay Switch Assembly, "RLDA" stands for Refrigerant Line Deployment Assembly, and "BPV" stands for Bypass Valve. "HSA REC" is the lowest temperature recuperator, and "OMS HX" is the low temperature heat exchanger providing the interface to the load from the focal plane modules.

shield heat exchanger and on the refrigerant lines. The new requirements change the balance between the "18 K" and 6.2 K loads and represent an overall load increase. For small changes near the previous operating point, the relative effect on required input power of heat at 6.2 K is approximately six times that of the same amount of heat at 18 K (see Figure 5 of Durand, et al.,[4] for example). With no other changes, the reduction of 13 mW at 6.2 K would be expected to enable an increase of roughly 78 mW at 18 K. The increase in 18 K load of 153 mW is nearly twice that.

The J-T and PT compressors are each driven by a dedicated Cryocooler Control Electronics (CCE) unit. There are no changes to the design of either the J-T-CCE or the PT-CCE required to adapt to the changed requirements. As has been the case, both CCEs are redundant, connected to their respective compressor through the Relay Switch Assembly (RSA).

COOLER SUBSYSTEM PERFORMANCE TESTING

Functional performance testing of the Development Model (DM) cooler was similar to that used to demonstrate Technology Readiness Level Six (TRL 6), as described by Durand.[3] Key hardware changes from the prior testing include replacing the pulse tube precooler with the one used to validate the reproducibility of the design (see Durand.[4]), replacing the laboratory version of the Joule-Thomson compressor with a higher fidelity, flight-like prototype, and changing the J-T restriction to allow higher mass flow through the J-T loop. The performance of the pulse tube precooler is described in detail in Durand.[4] In addition to design and construction consistent with flight hardware, the prototype Joule-Thomson compressor incorporates internal design changes leading to an increase in efficiency, at the compressor level, of approximately 25-30%. Figure 2 shows the prototype valved compressor. The J-T restriction design remains unchanged, just the defining dimension was changed to allow the higher mass flow rate. Other pieces of hardware from the TRL 6 testing series have been replaced with no intentional change in thermodynamic performance.

Performance testing is conducted in a complete "end-to-end" test with the PT precooler, recuperator, line representing the length of the RLDA, remote recuperator and all cold J-T hardware in a 36 inch bell-jar vacuum chamber with cooled shields to provide the low background temperature for hardware to be located in the cold environment inside the Integrated Science Instrument Module (ISIM) in the application. Resistive heaters are used to apply explicit heat loads and simulate parasitic loads.

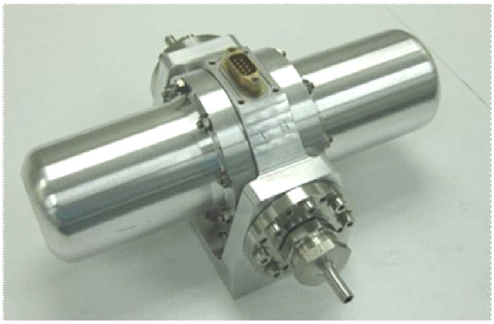

Figure 2. Flight-like prototype valved compressor used to circulate helium gas in the Joule-Thomson cooling loop.

Figure 1 shows the highest performing approach to adding a thermal interface for the actively cooled shield; the addition of the shield heat exchanger. It is also possible to provide cooling to the shield by attaching it with a conductive strap to the structure of the HSA at a somewhat degraded performance. In the test, either configuration can be simulated by applying the heat to the appropriate heaters. For the heat exchanger design, all the shield heat is applied to the return refrigerant line. The design utilizing a conductive strap to the structure of the HSA was simulated by applying the specified shield heat load to the supply line. Both approaches were tested.

RESULTS

Cooling lift at the OM heat exchanger was measured as a function of temperature, both in the initial cooldown, or “bypass” mode where the precooled helium gas bypasses the Joule-Thomson restriction and passes directly through the OM heat exchanger, and in the Joule-Thomson mode. Heat is applied to the resistive heaters in close thermal contact with the refrigerant lines and the HSA structure during the test to represent the 18 K and line loads. The equivalent of 475 W of bus power is applied during the cool-down, and data is taken near the steady state temperature with the equivalent of 400 W applied. From this data the maximum OM heat exchanger load at the pinch point and at steady state, corresponding to full bus power, is measured. The thermal rejection temperature of the PT precooler is controlled with an actively controlled liquid cooled heat exchanger.

Table 1 shows the measured heat load on the transfer lines, equivalent to the sum of the load from the actively cooled shield and the parasitic load on the lines, and the cooler’s lift at the OM heat exchanger for the pinch point and steady state for both design options for providing the shield interface, the thermal strap and the heat exchanger. In each case, two measurements are made, one with the applied line load below the required value and the other with the line load above the requirement, to enable accurate interpolation to the OM lift at the actual required line load value.

These measured performance values meet the requirements for the MIRI Cooler application. Using a heat exchanger to provide the thermal interface to the actively cooled shield provides improved performance over the use of a thermal strap.

CONCLUSION

The measurements reported here demonstrate the ability of the MIRI Cooler design to meet the modified cooling requirements, corresponding to changes in the overall MIRI and ISIM cryogenic design, including the addition of an actively cooled thermal intercept shield around the MIRI Optical Module. The net effect of the cryogenic system design changes and the newly demonstrated cooler capability is an increase in the overall margin of cooling capability over the expected thermal loads.

The thermodynamic model of the MIRI Cooler, anchored in measurements made during the demonstration of Technology Readiness Level Six (TRL 6), was used to predict cooler performance in the range of operating conditions beyond any the cooler had been characterized to previously.

Table 1. Measured MIRI DM Cooler performance data points, left, consisting of two measurements near each required condition to characterize the local slope of OM heat lift as a function of line load and the extrapolated value at the required line load value, right. Measurements are made for each required condition, Pinch Point and Steady State for the heat exchanger approach, indicated by "HX," and for the passive thermal strap approach, indicated by "Strap." The limiting case where the line loads go to zero are also shown for reference. When the line loads are zero, there is no difference between the "Strap" and "HX" configuration, the data is simply repeated to provide a data set for each configuration.

Measured							Extrapolated to current requirements			
Mode	**Line Load**	**OM Lift**	**OM Temp**	**HSA T**	**Bus Power**	**Trej**	**Local slope**	**Line Load**	**OM Lift**	**OM req**
Strap at Pinch Point							**Strap at Pinch Point**			
Strap PP	239mW	**52mW**	19.9K	20.0K	476 W	310K	-0.110mW/mW	203.1mW	**56.1mW**	56.4mW
Strap PP	208mW	**56mW**	19.0K	19.2K	471 W	310K				
No Load PP	0mW	**97mW**	15.2K	13.9K	470 W	310K				
Strap at Steady State							**Strap in Steady State**			
Strap SS	239mW	**72mW**	6.2K	22.0K	400 W	306K	-0.164mW/mW	232.3mW	**73.6mW**	55.2mW
Strap SS	208mW	**78mW**	6.2K	21.3K	400 W	306K				
No Load SS	0mW	**113mW**	6.2K	17.2K	395 W	307K				
HX at Pinch Point							**HX at Pinch Point**			
HXPP	241mW	**58mW**	19.1K	19.2K	475 W	310K	-0.160mW/mW	203.1mW	**63.8mW**	56.4mW
HXPP	208mW	**63mW**	18.3K	18.4K	476 W	310K				
No Load PP	0mW	**97mW**	15.2K	13.9K	470 W	310K				
HX at Steady State							**HX at Steady State**			
HXSS	241mW	**75mW**	6.2K	21.7K	400 W	306K	-0.159mW/mW	232.3mW	**76.2mW**	55.2mW
HXSS	208mW	**81mW**	6.2K	20.9K	400 W	306K				
No Load SS	0mW	**113mW**	6.2K	17.2K	395 W	307K				

The model included the behavior of the thermal rejection system connected to the hot-side thermal interface of the pulse tube precooler. A flight-like prototype Joule-Thomson compressor, replacing the laboratory version used in the TRL 6 testing performed previously, demonstrated increased thermodynamic efficiency. Adjusting the cooler design and operating conditions, using essentially unchanged components including the entire pulse tube precooler, the Joule-Thomson compressor and recuperators, and the cryocooler control electronics driving the pulse tube precooler and Joule-Thomson compressor, we were able to demonstrate in test the newly defined performance requirements. In addition to successfully adapting the design and operating parameters to meet the requirements for the MIRI/JWST mission, the design and modeling tools enable reliable performance predictions for other space-based astronomy applications.

ACKNOWLEDGMENT

This work is funded by NASA and managed by the California Institute of Technology, Jet Propulsion Laboratory.

REFERENCES

1. D. Durand, J. Raab, R. Colbert, M. Michaelian, T. Nguyen, M. Petach, and E. Tward, "NGST Advanced Cryocooler Technology Development Program (ACTDP) Cooler System," *Adv. in Cryogenic Engineering*, Vol. 51, Amer. Institute of Physics, Melville, NY (2006), pp. 615-622.
2. D. Durand, R. Colbert, C. Jaco M. Michaelian, T. Nguyen, M. Petach, and E. Tward, " NGST Advanced Cryocooler Technology Development Program (ACTDP) Cooler System in the 14th International Cryocooler Conference," *Cryocoolers 14,* ICC Press, Boulder, Colorado (2007), pp. 21-29.
3. D. Durand, R. Colbert, C. Jaco M. Michaelian, T. Nguyen, M. Petach, and J. Raab, "Mid InfraRed Instrument (MIRI) Cooler Subsystem Prototype Demonstration", *Adv. in Cryogenic Engineering*, Vol. 53, Amer. Institute of Physics, Melville, NY (2008), pp. 807-814.
4. D. Durand, D. Adachi, D. Harvey C. Jaco, M. Michaelian, T. Nguyen, M. Petach, and J. Raab, "Mid InfraRed Instrument (MIRI) Cooler Subsystem Design," *Cryocoolers 15,* ICC Press, Boulder, Colorado (2009), pp. 7-12.